Purton Louise (Orcid ID: 0000-0001-6593-3168)
Wu Joy Y. (Orcid ID: 0000-0002-1897-4503)

Loss of parathyroid hormone receptor signaling in osteoprogenitors is associated with accumulation of multiple hematopoietic lineages in the bone marrow

Takaharu Kimura, MD, PhD[1], Cristina Panaroni, PhD[1], Erinn B Rankin, PhD[2], Louise E. Purton, PhD[3,4], Joy Y. Wu, MD, PhD[1]

Departments of [1]Medicine (Endocrinology) and [2]Radiation Oncology, Stanford University School of Medicine, Stanford, CA. [3]St Vincent's Institute of Medical Research, Fitzroy, Victoria, Australia and [4]The University of Melbourne, Department of Medicine at St Vincent's Hospital, Fitzroy, Victoria, Australia.

Running title: PTH1R regulates hematopoietic cell trafficking

Corresponding author:
Joy Y. Wu, MD, PhD
300 Pasteur Dr., S-025
Stanford, CA 94305
TEL: 650-736-9654
Email: jywu1@stanford.edu

This is the author manuscript accepted for publication and has undergone full peer review but has not been through the copyediting, typesetting, pagination and proofreading process, which may lead to differences between this version and the Version of Record. Please cite this article as doi: 10.1002/jbmr.4568

Disclosures: None.

Data Availability Statement: The data that support the findings of this study are openly available in the NCBI Gene Expression Omnibus (accession number GSE185944).

Abstract

Osteoblasts and their progenitors play an important role in the support of hematopoiesis within the bone marrow microenvironment. We have previously reported that parathyroid hormone receptor (PTH1R) signaling in osteoprogenitors is required for normal B cell precursor differentiation, and for trafficking of maturing B cells out of the bone marrow. Cells of the osteoblast lineage have been implicated in the regulation of several other hematopoietic cell populations, but the effects of PTH1R signaling in osteoprogenitors on other maturing hematopoietic populations have not been investigated. Here we report that numbers of maturing myeloid, T cell, and erythroid populations were increased in the bone marrow of mice lacking PTH1R in osteoprogenitors (PTH1R-OsxKO mice). This increase in maturing hematopoietic populations was not associated with an increase in progenitor populations or proliferation. The spleens of PTH1R-OsxKO mice were small with decreased numbers of all hematopoietic populations, suggesting that trafficking of mature hematopoietic populations between bone marrow and spleen is impaired in the absence of PTH1R in osteoprogenitors. RNA sequencing of osteoprogenitors and their descendants in bone and bone marrow revealed increased expression of VCAM-1 and CXCL12, factors that are involved in trafficking of several hematopoietic populations.

Key words: PTH/Vit D/FGF23, Osteoblasts, Stromal/Stem Cells, Osteoimmunology, Genetic animal models

Introduction

Within the bone marrow microenvironment, parathyroid hormone (PTH) receptor signaling in the osteoblast lineage plays a crucial role in supporting hematopoiesis [1]. Activation of the PTH receptor PTH1R in mature osteoblasts in mice increases trabecular bone and osteoblast numbers, accompanied by an increase in hematopoietic stem cells (HSCs) [2]. PTH injections enhance mobilization of HSCs into peripheral blood in both mice [3] and humans [4].

We have previously reported that PTH1R signaling is required in osterix (Osx)-expressing osteoprogenitors for early B cell precursor differentiation [5, 6]. PTH1R is also required for trafficking of immature B cells out of bone marrow. In mice lacking PTH1R in Osx-expressing osteoprogenitors (PTH1R-OsxKO mice), B cells are abnormally retained in the marrow, due at least in part to increased levels of vascular cell adhesion protein 1 (VCAM-1) [5]. PTH1R is a G protein-coupled receptor, and the stimulatory heterotrimeric Gs protein is an important mediator of the anabolic bone-building effects of PTH1R signaling [7, 8]. The $G_s\alpha$ subunit is also required in osteoprogenitors for normal B cell precursor differentiation [6].

Beyond HSCs and B cells, the osteoblast lineage influences other hematopoietic populations as well. Ablation of osteoblasts in mice leads to rapid loss of bone marrow erythroid progenitors [9], while stabilization of HIF in osteoprogenitors by conditional deletion of VHL leads to increased trabecular bone and polycythemia due to increased expression of erythropoietin in osteoblasts [10]. Ablation of mature osteocalcin-expressing osteoblasts in mice decreases T cell precursor numbers and impairs their differentiation in the thymus [11].

Expression of the $G_s\alpha$ subunit in osteocytes regulates neutrophils via production of G-CSF [12]. However, the role of PTH1R signaling in regulating other hematopoietic populations is unknown. Here we report that myeloid, T cell, and late erythroid populations were increased in the bone marrow of PTH1R-OsxKO mice, despite a profound decrease in proliferation, while all hematopoietic populations were significantly decreased in the spleen of PTH1R-OsxKO mice.

Transcriptome profiling of PTH1R-OsxKO osteoprogenitors and littermate controls revealed changes in several niche factors that may regulate trafficking of hematopoietic cells between bone marrow and spleen.

Material and Methods

Mice

Mice lacking PTH1R in osteoprogenitors [5] were generated by mating $PTH1R^{fl/fl}$ mice in which loxP sites are placed in the introns flanking the essential E1 exon [13], with Osx-GFP::Cre transgenic mice in which Cre recombinase is fused to green fluorescent protein (GFP), under the control of the promoter for osterix, a transcription factor expressed early in osteoblastogenesis [14]. $PTH1R^{fl/fl}$ littermates were used as controls for all experiments unless otherwise stated. Although the presence of Osx-driven Cre recombinase transgene results in mild runting, it is not associated with a hematopoietic phenotype [5]. There is no difference in phenotypes between $PTH1R^{fl/fl}$ and $PTH1R^{+/+}$ mice [5]. Genotyping was performed on genomic DNA obtained from tail biopsies as previously described [5]. All animals were housed in Innovive recyclable individually ventilated cages in a designated pathogen-free area facility and fed irradiated mouse chow and autoclaved water. The Veterinary Service Center at Stanford University provides laboratory animal care and is administered by the Department of Comparative Medicine. The laboratory animal care program at Stanford University is fully accredited by the Association for Accreditation and Assessment of Laboratory Animal Care. All procedures were approved by the Stanford University Administrative Panel on Laboratory Animal Care.

Ai14 reporter mice have a loxP-flanked STOP cassette preventing transcription of a CAG promoter-driven red fluorescent protein variant (tdTomato), all inserted into the Gt(ROSA)26Sor locus, and were obtained from the Jackson Laboratory (stock no. 007908). Ai14 mice express robust tdTomato fluorescence following Cre-mediated recombination.

Mice lacking PTH1R in mesenchymal progenitors were generated by mating PTH1R(fl/fl) mice to transgenic mice in which Cre recombinase is driven by the leptin receptor promoter (from the Jackson Laboratory, stock no. 008320) [15, 16].

Flow cytometry

Femur, tibia and spleen were harvested from sacrificed mice. Bone marrow (BM) hematopoietic cells were isolated by flushing, and spleen hematopoietic cells were crushed through 100 µm cell strainers (BD Biosciences). Nucleated cells were counted in Turk's solution (Sigma-Aldrich) according to the manufacturer's protocol. Erythroid cell, including erythrocyte lineage absolute numbers were determined using Precision Count Beads (BioLegend). To obtain BM stroma cells, flushed BM was digested with 1 mg/ml collagenase IV (Gibco) and 2 mg/ml dispase II (Sigma-Aldrich) for 30 min. at 37°C. To obtain bone cells, BM-flushed bones were chopped into small pieces, then digested with 0.5 mg/ml collagenase type I and 1.5 mg/ml collagenase type II (Worthington) solution for 90 minutes at 37°C. Harvested cells were filtered through 100 µm cell strainer and stained with antibodies (Supplementary Table 1). For intracellular FoxP3 staining cells were fixed and permeabilized using the Anti-Mouse/Rat Foxp3 Staining Set (eBioscience), then stained with APC-conjugated anti-Foxp3 antibody (eBioscience) [17]. Cells were analyzed and sorted using FACS Aria II (BD Biosciences). Data were analyzed using Flowjo software (version 10.7.1).

Immunostaining

Femurs and spleens were freshly isolated or fixed with 4% paraformaldehyde, then embedded into super cryoembedding medium (SCEM, Section-Lab) and frozen. Sections were prepared and immunostained according to the Kawamoto method [18]. Immunofluorescence images were acquired by LSM 780 confocal microscopy and analyzed with ZEN software (Carl Zeiss). The markers and antibodies were used as follows: DAPI (Sigma-Aldrich), a DNA marker; Alexa488-conjugated anti-mouse Ter119, Alexa594-conjugated anti-mouse B220, Alexa647-conjugated Streptavidin (BioLegend); Biotin-conjugated anti-mouse Ki-67 (eBioscience); chicken

anti-GFP (Aves Labs); goat anti-CD31 (R&D Systems); CF488A-conjugated donkey anti-chicken IgY, CF647-conjugated donkey anti-goat IgG (Sigma-Aldrich).

Colony forming assays

BM or Spleen cells were suspended in 3 mL of MethoCult SF M3436 medium (StemCell Technologies) for burst-forming unit-erythroid (BFU-E) or MethoCult M3334 (StemCell Technologies) for colony-forming unit-erythroid (CFU-E) assays, then plated into three 35-mm dishes (StemCell Technologies) and incubated in 5% CO_2 at 37°C. After 48 hours for CFU-E and 10 days for BFU-E, the plates were scored using an EVOS Imaging System (Thermo Fisher Scientific).

Cell cycle analysis

Hematopoietic cells were stained with cell surface antigens, then fixed and permeabilized using Cytofix/Cytoperm Fixation/Permeabilization Solution Kit (BD Biosciences). The cells were stained with PE-conjugated anti-mouse Ki-67 (BioLegend) and Hoechst 33342 (Sigma-Aldrich) and analyzed by FACS Aria II.

RNA sequencing

For bulk cell RNA sequencing, total RNAs were extracted from sorted cells with the RNeasy Plus Micro Kit (Qiagen), then libraries were prepared with the SMART-Seq v4 Ultra Low Input RNA Kit for Sequencing and SMARTer ThruPLEX DNA-Seq Kit (Takara Bio). Library quality was verified using the Agilent High Sensitivity DNA Kit on Agilent's 2100 Bioanalyzer. For each library, average 350 bp fragments were sequenced using paired end reads (2 × 100 bp) on the HiSeq 4000 platform (Stanford Personalized Medicine Sequencing Core), with an average of 20 million reads per sample. Paired end sequencing reads (100bp) were generated and aligned to the mouse reference sequence NCBI Build 38/mm10 with the STAR (v2.4.2a) algorithm [49]. Normalization of RefSeq annotated gene expression level and differential expression analysis were performed using Bioconductor package DESeq2 in R (Version 3.2.2) [50]. Rlog transformed values (the regularized-logarithm transformation for count data) was calculated for each gene.

Genes with False Discovery Rate (FDR) < 0.05 were defined as differentially expressed genes. Gene ontology analysis was performed at Gene Ontology Consortium (http://geneontology.org/). All transcriptome raw data are publicly available in the NCBI Gene Expression Omnibus (accession number GSE185944).

Statistics

Statistical analyses were performed using two-tailed, unpaired Student's t test in GraphPad Prism 9 (GraphPad Software, San Diego, CA). Quantitative data are presented as boxplot with maximum and minimum whiskers or mean ± SEM.

Results

PTH1R signaling in osteoprogenitors influences maturing myeloid, T cell, and erythroid lineages

To examine the role of PTH1R signaling in skeletal and hematopoietic development, mice lacking PTH1R in Osx-expressing osteoprogenitors (PTH1R-OsxKO mice) were derived by crossing Osx-Cre::GFP transgenic mice with $PTH1R^{fl/fl}$ mice as previously described [5]. In the absence of doxycycline, the Cre recombinase is constitutively expressed in Osx+ osteoprogenitors throughout embryonic development. As we have previously published, conditional knockout mice were born at the expected Mendelian ratio but were smaller than control littermates and did not survive past 1 month of age, for unknown reasons. As a result all analyses were carried out before postnatal day 21 [5]. Since we have demonstrated that expression of the Osx-Cre::GFP transgene does not significantly impact the hematopoietic phenotype [5], $PTH1R^{fl/+}$ and $PTH1R^{fl/fl}$ littermate mice were used as controls unless otherwise specified. We have previously reported that when adjusted for decreased body weight, bone marrow cellularity is increased in PTH1R-OsxKO mice, while spleen cellularity and spleen weight

are significantly decreased in PTH1R-OsxKO mice even when adjusted for decreased body weight [5].

Myeloid (B220-CD11b+CD3-Ter119-) and T cells (B220-CD11b-CD3+Ter119-) were increased in PTH1R-OsxKO bone marrow, while B cells (B220+CD11b-CD3-Ter119-) were decreased, and there was no change in the numbers of erythroid cells overall (B220-CD11b-CD3-Ter119+) (Figure 1A). In the spleen, all hematopoietic populations were decreased in PTH1R-OsxKO mice (Figure 1A). Given the dramatic decline in hematopoietic populations in the spleen, we sought to determine whether the Osx-Cre::GFP transgene might be ectopically expressed in the spleen at day 21. While GFP expression, which marks cells currently expressing the Osx-Cre::GFP transgene, is detectable in bone at day 21, no GFP is detectable in the spleen (Supplementary Figure 1).

Within the myeloid lineage, granulocyte (CD3-CD19-Ter119-CD11b+Ly6G+SiglecF-), monocyte/macrophage (CD3-CD19-Ter119-CD11b+Ly6G-SiglecF-), and eosinophil (CD3-CD19-Ter119-CD11b+SiglecF+) subpopulations were all increased in PTH1R-OsxKO bone marrow (Figure 1B). In the spleen granulocyte and monocyte/macrophage subpopulations were decreased in PTH1R-OsxKO mice (Figure 1B).

Within the T cell lineage, CD4 (CD4+CD8-Foxp3-), CD8 (CD4-CD8+Foxp3-), and regulatory T cells (CD4+Foxp3+) [19] were increased in PTH1R-OsxKO bone marrow (Figure 1C). In the spleen all T cell populations were decreased in PTH1R-OsxKO mice (Figure 1C).

Within the erythroid lineage, stage I through IV differentiating erythroblasts can be distinguished based on expression of Ter119 and progressive loss of CD71 (transferrin receptor) (Supplementary Figure 2A) [20, 21]. Stage I and stage IV erythroblasts were increased in PTH1R-OsxKO bone marrow (Figure 1D). In the spleen all 4 stages of erythroblasts were decreased in PTH1R-OsxKO mice (Figure 1D). Using another erythroid lineage phenotyping protocol that captures terminal erythroid differentiation (Supplementary Figure 2B) [22], erythroblast stages I

and IV (proerythroblasts and orthochromatic erythroblasts, respectively), and erythrocyte stages V and VI (reticulocytes and erythrocytes, respectively), were increased in PTH1R-OsxKO mice (Supplementary Figure 2C). In the spleen the numbers of all erythroblast/erythrocyte stages were decreased in PTH1R-OsxKO mice (Supplementary Figure 2C). Therefore mature myeloid, T and erythroid lineage populations were all increased in PTH1R-OsxKO bone marrow, as we have previously reported for maturing B cells [5].

To determine whether the increase in maturing hematopoietic populations in the bone marrow is associated with changes in the circulation, we assayed complete blood counts on peripheral blood from control and PTH1R-OsxKO mice. There were no differences in red blood cells (RBCs), hemoglobin or hematocrit between PTH1R-OsxKO and control mice, but mean corpuscular volume (MCV) was slightly, and significantly, decreased in PTH1R-OsxKO blood (Figure 1E). Circulating white blood cells (WBCs) were significantly decreased in PTH1R-OsxKO mice, accompanied by an increased frequency in neutrophils and a reduced frequency of lymphocytes, the latter consistent with our previous study that revealed an impaired egress of B lymphocytes from the bone marrow (Figure 1F) [5]. There was no difference in platelet counts between PTH1R-OsxKO and control mice (Figure 1G).

Hematopoietic progenitors are unaffected

To determine whether the increase in maturing hematopoietic populations in the bone marrow is associated with an increase in progenitors, we analyzed by flow cytometry hematopoietic stem/progenitor cell populations, the majority of which are located in the center of the marrow and depleted near the bone surface [23]. We found no differences in the numbers of long-term HSCs (LT-HSC, CD150+CD48-Lin-c-kit+Sca-1+) [24], short-term HSCs (ST-HSC, CD34+Flt3-Lin-c-kit+Sca-1+) [25], lymphoid-primed MPPs (LMPP, CD34+Flt3+Lin-c-kit+Sca-1+) [26], common lymphoid progenitors (CLP, CD127+Lin-c-kit+Sca-1+) [27], common myeloid progenitors (CMP, CD34+CD16/32-Lin-c-kit+Sca-1-), megakaryocyte-erythrocyte progenitors (MEP, CD34-CD16/32-Lin-c-kit+Sca-1-), or granulocyte-monocyte progenitors (GMP, CD34+CD16/32+Lin-c-kit+Sca-1-)

[28] in the bone marrow (Figure 2A). In the spleen the numbers of ST-HSC, LMPP, CLP, CMP, and MEP were all decreased in KO mice (Figure 2A).

The numbers of pre-granulocyte-monocyte progenitors (pre-GM, CD41-CD16/32-CD150-CD105-), granulocyte-macrophage progenitors (GMP, CD41-/CD150-/CD16/32+), pre-MegE (CD41-CD16/32-CD150+CD105-) and pre-CFU-E (CD41-CD16/32-CD150+CD105+) did not differ between control and PTH1R-OsxKO bone marrow [29]. There was a significant increase in the numbers of CFU-E (CD41-CD16/32-CD150-CD105+Ter119-), pro-Ery (CD41-CD16/32-CD150-CD105+Ter119+) and megakaryocyte progenitors (MkP, CD41+ CD150+) in PTH1R-OsxKO bone marrow (Figure 2B). In the spleen the numbers of pre-GM, pre-MegE, pre-CFU-E, CFU-E, pro-Ery and MkP were all decreased in PTH1R-OsxKO mice (Figure 2B). In CFU assays there was no difference in CFU-E in either bone marrow or spleen (Figure 2C). There was no difference in BFU-E in bone marrow, while BFU-E are increased in KO spleen.

Unlike other hematopoietic populations, T cells are derived from bone marrow common lymphoid progenitors but mature in the thymus. We also examined T cell precursor populations in the thymus. Thymus weight, both absolute and corrected for body weight, was decreased in PTH1R-OsxKO mice (Figure 2D). Thymus cellularity was decreased but there was no difference when corrected for body weight. Within the thymus there were no differences in the numbers of any of the T cell precursors: double negative (DN, Lin-CD4-CD8-), DN1 (Lin-CD4-CD8-CD25-CD44+), DN2 (Lin-CD4-CD8-CD25+CD44+), DN3 (Lin-CD4-CD8-CD25+CD44-), DN4 (Lin-CD4-CD8-CD25-CD44-), double positive (DP, Lin-CD4+CD8+), CD4 single positive (SP, Lin-CD4+CD8-) and CD8 SP (Lin-CD4-CD8+) (Figure 2E).

Proliferation of hematopoietic populations is decreased

The increase in mature populations in the bone marrow is not driven by increased numbers of progenitors. We therefore performed cell cycle analyses by flow cytometry. In the bone marrow we found a striking decrease in the proportion of cells in G2/M/S cell cycle phases in all

lineages, with an increased proportion of cells in the quiescent G0 state among all populations except myeloid cells (Figure 3A). In the spleen, the proportion of cells in G2/M/S phases of the cell cycle were decreased for myeloid, T and B cell lineages. In maturing erythroblasts there was a dramatic increase in the proportion of cells in the quiescent G0 state and a decrease in the proportion of cells in G1 at all stages in the bone marrow of PTH1R-OsxKO mice. In the spleen the proportion of cells in the quiescent G0 state was increased in stage II erythroblasts while the proportion of cells in G2/M/S phases of the cell cycle was decreased in stage I-IV erythroblasts (Figure 3B).

Immunohistochemical staining of bone marrow for the proliferation marker Ki-67 in the femur confirmed a decrease in proliferating Ter119$^+$ erythroid lineage cells (Figure 3C). In the spleen there was a decrease in Ter119$^+$ and Ki-67$^+$ cells, and impaired organization of B220$^+$ B lymphoid lineage cells into follicles (Figure 3D). Therefore the accumulation of mature hematopoietic populations in the bone marrow is not due to an increase in proliferation. Instead, the proliferation of almost all hematopoietic populations is strikingly decreased in PTH1R-OsxKO bone marrow and spleen.

PTH1R signaling in mesenchymal stem/progenitor cells does not influence hematopoiesis

Studies suggest that within the bone marrow microenvironment, mesenchymal stem/progenitor cells expressing leptin receptor (LepR) and osteoprogenitors expressing Osx serve distinct roles in the hematopoietic niche. For example, deletion of CXCL12 in LepR$^+$ mesenchymal progenitor cells affects hematopoietic stem/progenitor cells [30], while deletion of CXCL12 in Osx$^+$ osteoprogenitors affects CLPs and pre-pro-B cells [31]. Deletion of SCF in LepR$^+$ cells leads to loss of HSPCs, while deletion in committed osteoblasts does not [16]. We have also reported that PTH1R is required in osteoprogenitors, but not mature osteoblasts or osteocytes, for normal B cell precursor development [5].

To determine whether PTH1R is required in mesenchymal stem/progenitor cells to support maturing hematopoietic lineages, we examined PTH1R-LepRKO mice lacking PTH1R in LepR$^+$ mesenchymal stem/progenitor cells. At the beginning of the COVID-19 pandemic as research laboratories were abruptly closed it became necessary to significantly reduce the size of our mouse colony. Due to lack of apparent phenotype (see below) the PTH1R-LepRKO line was therefore eliminated. Because we did not confirm reduced *Pth1r* expression in LepR+ cells, these results are included only as supplementary data. LepR expression has been reported in murine perivascular stromal cells at 3-4 months of age [32]. We therefore examined PTH1R-LepRKO and control mice at 3 months of age and found no differences in body weight, bone marrow cellularity, spleen weight, or spleen cellularity (Supplementary Figure 3A). There was an increase only in the number of erythroid cells that is restricted to erythroblast stage IV [20, 21] in the bone marrow of KO mice (Supplementary Figure 3B), indicating that PTH1R expression in LepR$^+$ cells does not noticeably affect myeloid, or T cell populations and has minimal effects on the erythroid lineage in the bone marrow. There were no differences in hematopoietic populations in the spleen. Therefore PTH1R in LepR$^+$ stromal cells is not required for normal myeloid, B, and T lineage differentiation at 3 months.

Over time LepR$^+$ stromal cells give rise to osteoblasts in adult mice. While at 6 months of age fewer than 25% of osteoblasts are derived from LepR$^+$ precursors, by 14 months a majority (61-81%) of osteoblasts are derived from LepR$^+$ precursors [32]. The differentiation of LepR$^+$ precursors to mature osteoblasts progresses through an Osx-expressing stage [33]. To determine whether PTH1R in the osteoblast lineage affects hematopoiesis in older adult mice, we examined PTH1R-LepRKO mice at 12 months of age, when the majority of osteoblasts are expected to have descended from LepR-Cre cells [32]. There were no differences in body weight, bone marrow cellularity, spleen weight, or spleen cellularity between PTH1R-LepRKO and control mice (Supplementary Figure 3C). In the bone marrow there was a decrease only in the number of myeloid cells (Supplementary Figure 3D). There were no differences in other hematopoietic lineages, and the spleen was not affected. Therefore PTH1R signaling in LepR-

expressing cells and their mesenchymal progeny has only a very modest effect on hematopoiesis.

Differential expression of candidate niche factors

In PTH1R-OsxKO and PTH1R$^{+/+}$; Osx-Cre::GFP/+ (PTH1R-OsxWT) mice, the osterix promoter drives expression of both Cre recombinase and green fluorescent protein (GFP), so GFP expression marks cells that currently express osterix. To examine the effects of loss of PTH1R in osteoprogenitors on their progeny we crossed PTH1R-OsxKO and PTH1R-OsxWT mice to Ai14 Tm$^+$ reporter mice that express robust tdTomato (Tm) fluorescence following Cre-mediated recombination, so Tm expression marks cells that have descended from Osx-expressing cells. Immunostaining reveals that GFP$^+$ cells were detectable in bone (bone-current, representing immature osteoprogenitors), while Tm$^+$ cells were detectable in both bone (bone-historic, encompassing mature osteoblasts, bone lining cells, and osteocytes) and bone marrow stroma (BM-historic, including perivascular mesenchymal cells) (Figure 4A). Analysis of GFP and Tm expression by flow cytometry confirmed that bone marrow contained only Tm$^+$ BM-historic cells, which were increased in PTH1R-OsxKO compared to PTH1R-OsxWT mice (Figure 4B-C). GFP$^+$ cells appeared infrequent by immunostaining in the bone, but by flow cytometry numbers of GFP$^+$ bone-current cells were comparable to Tm$^+$ bone-historic cells in WT mice. In KO bone, the numbers of Tm$^+$ bone-historic cells were greater than GFP$^+$ bone-current cells.

To identify candidate niche factors that are differentially expressed in PTH1R-OsxKO mice we performed RNA-sequencing on osteoprogenitors and their descendants. We sorted bone-current, bone-historic and BM-historic cells from PTH1R-OsxKO and PTH1R-OsxWT mice and performed RNA-sequencing. Principal component analysis demonstrated that PC1 (encompassing 84% of variance) clearly distinguished bone-current, bone-historic, and BM-historic cells, while PC2 (7% variance) distinguished these populations by genotype (Figure 5A). This was confirmed by a heatmap which revealed clustering by cell population first with BM-historic the most distinct group, followed by genotype (Figure 5B). These data are consistent

with reports that Osx-expressing cells give rise to distinct populations in bone and bone marrow [34].

We have previously reported that maturing B cells accumulate in the bone marrow of PTH1R-OsxKO mice due to abnormal retention, mediated at least in part by increased levels of VCAM-1 [5]. The increase in myeloid subsets, T cells, and late erythroblasts in the bone marrow despite a marked decrease in proliferation suggests that these hematopoietic populations may also be abnormally retained in the bone marrow. Inspection of RNA-sequencing data confirmed that *Pth1r* mRNA was more highly expressed in PTH1R-OsxWT populations, while *Vcam1* mRNA levels were more highly expressed in PTH1R-OsxKO populations (Figure 5C). We examined cell surface expression of VCAM-1 and its primary ligand VLA-4 by flow cytometry and found increased expression of VCAM-1 among myeloid and B lymphoid populations in the bone marrow of PTH1R-OsxKO mice (Figure 5D). Of note, VLA-4 expression was significantly decreased among T lymphoid cells in the bone marrow of PTH1R-OsxKO mice.

CXCL12 is a chemokine that also plays a significant role in trafficking of HSPCs, lymphocytes, and myeloid cells [15, 35-37]. CXCL12 is increased in the bone marrow microenvironment of mice with constitutively active PTH1R targeted to osteoblasts [2]. Surprisingly, we found that *Cxcl12* expression was increased in PTH1R-OsxKO mice (Figure 5C). Inspection of RNA-sequencing data revealed that mRNA levels of *Cxcl12* were increased in all three populations. Therefore VCAM-1 and CXCL12 are candidate mediators for the accumulation of myeloid, T, and late erythroid populations in the bone marrow of PTH1R-OsxKO mice.

We next examined the RNA-sequencing data to identify additional transcripts that are differentially expressed in each population. The top 20 niche factors upregulated in each PTH1R-OsxWT population (BM-historic, bone-current, bone-historic) are shown in Figure 6A. Several niche factors were increased in all PTH1R-OsxWT BM-historic, bone-current, and bone-historic populations, including pleiotrophin (*Ptn)*, mesencephalic astrocyte-derived neurotropic factor (*Manf*), adipolin (*C1qtnf12*), aminoacyl tRNA synthetase-interacting multifunctional

protein 1 (*Aimp1*), neudesin (*Nenf*), and macrophage migration inhibitory factor (*Mif*). Adropin (*Enho)*, glucose-6-phosphate isomerase 1 (*Gpi1*), interleukin 17B (*Il17b*), *Il17d* and osteocrin (*Ostn*) were increased in PTH1R-OsxWT bone-current and bone-historic populations; meteorin-like (*Metrnl)*, tissue inhibitor of metalloproteinase-1 (*Timp1*), and galanin (*Gal*) were increased in PTH1R-OsxWT BM-historic and bone-historic populations; and bone morphogenetic protein 7 (*Bmp7l)* and osteolectin (*Oln*) were increased in PTH1R-OsxWT BM-historic and bone-current populations.

The top 20 niche factors upregulated in each PTH1R-OsxKO population (BM-H, bone-C, bone-H) are shown in Figure 6B. Vascular endothelial growth factor A (*Vegfa*), M-CSF (*Csf1*), *Bmp6*, and *Cxcl12* were increased in all PTH1R-OsxKO BM-historic, bone-current, and bone-historic populations. Angiotensinogen (*Agt*), *Bmp1,* adiponectin (*Adipoq*), transforming growth factor β 2 *(Tgfb2), Bmp8a*, and heparin-binding EGF-like growth factor *(Hbegf*) were increased in PTH1R-OsxKO bone-current and bone-historic populations; stem cell factor (*Kitl*) and *Bmp4* were increased in PTH1R-OsxKO BM-historic and bone-historic populations; and *Bmp2* was increased in PTH1R-OsxKO BM-historic and bone-current populations.

Discussion

In summary we find an increase in overall numbers of myeloid and T cells in the bone marrow of PTH1R-OsxKO mice. While there is no increase in overall erythroid cells, there is an increase in the numbers of cells at late erythroblast or erythrocyte stages. Along with our previously reported finding that maturing B cells are increased in PTH1R-OsxKO bone marrow [5], these findings indicate that maturing hematopoietic cells in multiple lineages accumulate in the bone marrow of PTH1R-OsxKO mice. This increase in numbers across multiple hematopoietic lineages occurs without any change in precursor populations and despite a dramatic decrease in proliferation. There is a striking decrease in the spleen size and cellularity of PTH1R-OsxKO mice even after correcting for reduced body weight. Together the findings suggest that trafficking of

multiple hematopoietic cell lineages from bone marrow to the spleen is impaired in PTH1R-OsxKO mice. Furthermore, the migration of mature T cells from the thymus to the bone marrow, but not spleen, is increased in PTH1R-OsxKO mice.

We have previously reported that immature IgM+ B cells and maturing IgM+/IgD+ and IgD+ B cells accumulate in PTH1R-OsxKO bone marrow due to abnormal retention mediated in part by increased expression of VCAM-1 [5]. Here we have performed RNA-sequencing on Osx-expressing osteoprogenitors and confirm that *Vcam1* mRNA is increased in both Osx-current and Osx-historic populations in bone and bone marrow of PTH1R-OsxKO mice. In addition to lymphocytes [38], VCAM-1 has also been implicated in the regulation of HSPCs [39] and erythrocytes [40]. By flow cytometry we also find that VCAM-1 is increased on myeloid and B cells in PTH1R-OsxKO marrow, while VLA-4, the ligand for VCAM-1, is decreased on T cells.

We have also reported that conversely PTH treatment decreases VCAM-1 expression in bone, and this contributes to the ability of PTH to inhibit breast cancer metastases to bone in mice [41]. Together these findings suggest that PTH1R signaling negatively regulates VCAM-1, although the mechanisms remain unknown. While *Vcam1* expression has been reported in osteoblasts [42, 43], a role for PTH in its regulation has not been well characterized. Although most commonly studied gene targets of PTH are positively regulated by PTH [44], *Sost* (which encodes the Wnt inhibitor sclerostin) is the most prominent example of a gene that is potently suppressed by PTH [45, 46]. Suppression of *Sost* by PTH is mediated by the histone deacetylase HDAC5, which binds to and inhibits MEF2C activity on the *Sost* enhancer [47, 48]. HDACs have also been reported to negatively regulate *Vcam1* [49, 50]. Therefore one possible mechanism is that PTH directly inhibits *Vcam1* expression via HDACs.

An alternative possibility is that PTH1R signaling indirectly regulates VCAM-1, and candidate mechanisms include Wnt signaling and inflammation. Canonical Wnt inhibits *Vcam1* expression in marrow stromal cells [51]. Wnt signaling is stimulated by PTH1R, which inhibits the Wnt inhibitor *Sost* [46]. In endothelial cells and smooth muscle cells, VCAM-1 is induced by

inflammatory mediators such as TNF-α and IL-1β [40, 52-54]. The PI3K, MAPK and NF-kB pathways have been implicated in the stimulation of VCAM-1 by inflammatory mediators [52, 53, 55]. Strikingly, we have found that expression of genes encoding TNF-α and IL-1β are upregulated in PTH1R-deficient osteoprogenitors (data not shown).

Another candidate mediator of BM retention of hematopoietic cells in PTH1R-OsxKO mice is CXCL12. The chemokine CXCL12 also regulates trafficking of multiple hematopoietic lineages [15, 35-37]. While CXCL12 has been reported to be positively regulated by PTH1R signaling [2], here we report that *Cxcl12* expression is unexpectedly increased in Osx-current and Osx-historic bone and bone marrow populations in PTH1R-OsxKO mice.

RNA-sequencing of osteoprogenitor populations reveals several cytokines and growth factors implicated in the hematopoietic niche that are differentially expressed in PTH1R-OsxKO and PTH1R-OsxWT mice. Several have described roles in osteogenesis including pleiotrophin [56], Timp1 [57], meteorin-like [58], osteolectin [59], adrenomedullin [60], and osteocrin [61, 62]. Particularly intriguing among these are pleiotrophin, which plays a role in bone marrow HSC maintenance [63], and osteolectin, plasma levels of which in humans correlate with hemoglobin levels [64, 65]. Osteolectin was recently reported to be induced by PTH and to partially mediate the anabolic effects of PTH on bone [66].

One of the most striking phenotypes in PTH1R-OsxKO mice is hyposplenia. The greatest reductions in spleen cellularity affect the B cell and erythroid lineages. One explanation for decreased spleen cellularity is aberrant retention in the bone marrow. We have previously shown that B cells retention in the bone marrow by VCAM-1 likely contributes to their decreased presence in the spleen, and this is consistent with the decrease in circulating lymphocytes in the blood. Interestingly, while there is an accumulation of late erythroblast stages in the marrow, there is somewhat surprisingly no difference in circulating RBCs.

In humans the spleen can support hematopoiesis under stress conditions when needed as a site of compensatory (extramedullary) hematopoiesis, for example in diseases such as myelofibrosis or osteopetrosis that impair the ability of the bone marrow to sustain hematopoiesis [67, 68]. Extramedullary hematopoiesis can also develop in the adult spleen, particularly in red pulp, in response to a variety of insults including G-CSF, bone marrow transplantation, chemotherapy, and irradiation [69]. In mice the spleen can support stress erythropoiesis in response to acute anemia [70], and is an active site of erythropoiesis in the first weeks after birth until steady-state erythropoiesis is established in the bone marrow [71].

The findings in the spleen are in striking contrast to the thymus, where T cell precursor differentiation appears to proceed normally in PTH1R-OsxKO mice. Early T cell precursors, derived from common lymphoid progenitors, differentiate in the thymus into mature CD4 and CD8 T cells. Thymus weight and cellularity (corrected for body size) are unaffected in PTH1R-OsxKO mice. Common lymphoid progenitors are not decreased in PTH1R-OsxKO bone marrow, and differentiation of early T cell precursors appears to occur normally in both PTH1R-OsxKO and control mice. There is, however, a striking accumulation of mature CD4, CD8 and regulatory T cells within the bone marrow. Therefore lymphoid progenitors are apparently able to seed the thymus, where early precursor differentiation occurs normally, but mature T cells that circulate back to the bone marrow appear to be retained there.

The difference between thymus and spleen in PTH1R-OsxKO mice raises the possibility that there may also be intrinsic defects in the spleen microenvironment of PTH1R-OsxKO mice. In Gsa-OsxKO mice with impaired PTH1R signaling in osteoprogenitors, spleen size is markedly reduced at one week of age. While deletion of PTH1R by Osx-GFP:Cre should be limited to osteoprogenitors in the bone marrow, there remains the possibility that ectopic expression of Osx-GFP:Cre might occur in the spleen. A recent careful examination of extra-skeletal tissues revealed Osx expression in the olfactory bulb and gastric and intestinal cells, but did not examine the spleen [72]. As a surrogate marker for expression of the Cre recombinase we found no Osx-GFP expression in the spleen at 21 days of age, indicating little or no ongoing Osx

promoter-driven expression in the spleen. Future lineage tracing studies with a reporter for historic Cre expression will be required to conclusively determine whether Osx is expressed in the spleen earlier in development.

Studies on the bone marrow microenvironment have demonstrated that osteoblast lineage cells at varying stages of differentiation play unique roles in supporting hematopoiesis. For example, CXCL12 and SCF are required in LepR+ mesenchymal progenitors to support HSPCs [16, 30]. In contrast, CXCL12 in Osx+ osteoprogenitors is required to support early B cell precursors [31]. We have published that PTH1R is required in Osx+ osteoprogenitors but not maturing osteoblasts for early B cell precursor differentiation [5]. Here we report that PTH1R is not required in LepR+ mesenchymal progenitors to support maturing hematopoietic populations. These are consistent with reports that LepR+ stromal cells in young adult mice do not overlap with Osx+ cells [33], and is further supported by recent single-cell profiling studies of the bone marrow microenvironment [73, 74]. An important caveat is that we did not confirm Cre recombinase-mediated rearrangement of the *Pth1r* floxed allele before eliminating this line during the pandemic-imposed laboratory closure.

The relevance of osteoblast support of hematopoiesis has become increasingly apparent in humans. Bone loss is a clinical feature of several diseases associated with anemia, including sickle cell disease and thalassemia [75, 76]. We have demonstrated that bone loss is associated with anemia, decreased lymphocytes, and increased neutrophils in older men [77], and anemia is associated with an increased risk of fracture [78]. Once daily PTH administration in postmenopausal women with osteoporosis increases circulating HSCs in the blood [4].

In summary the loss of PTH1R signaling in osteoprogenitors within bone and bone marrow has a profound effect with increased hematopoietic mature populations within the bone marrow, and markedly decreased cellularity in the spleen, suggesting impaired trafficking between these organs. The mechanisms that regulate hematopoietic cell trafficking between bone marrow and

spleen are poorly defined but have significant clinical relevance. Understanding these mechanisms has clinical implications for immunity, anemia, and hematopoietic malignancies.

Acknowledgements

TK, CP and JYW were supported by funding from the National Institutes of Health [R56 DK112869 and R01 AR073773]. LEP was supported by a Senior Research Fellowship from the National Health and Medical Research Council (GNT1003339) and funding from the Victorian State Government Operational Infrastructure Support Program (to St. Vincent's Institute of Medical Research).

Contributions

Experiments were conceived and designed by TK, ER, LEP and JYW. The experiments were performed by TK and CP. All authors analyzed and interpreted the data. The paper was written by TK and JYW, with input from all authors.

References

1. Panaroni C, Tzeng YS, Saeed H, and Wu JY. Mesenchymal progenitors and the osteoblast lineage in bone marrow hematopoietic niches. Curr Osteoporos Rep 2014; 12(1):22-32.
2. Calvi LM, Adams GB, Weibrecht KW, Weber JM, Olson DP, Knight MC, . . . Scadden DT. Osteoblastic cells regulate the haematopoietic stem cell niche. Nature 2003; 425(6960):841-6.
3. Adams GB, Martin RP, Alley IR, Chabner KT, Cohen KS, Calvi LM, . . . Scadden DT. Therapeutic targeting of a stem cell niche. Nat Biotechnol 2007; 25(2):238-43.
4. Yu EW, Kumbhani R, Siwila-Sackman E, DeLelys M, Preffer FI, Leder BZ, and Wu JY. Teriparatide (PTH 1-34) Treatment Increases Peripheral Hematopoietic Stem Cells in Postmenopausal Women. J Bone Miner Res 2014; 29(6):1380-6.
5. Panaroni C, Fulzele K, Saini V, Chubb R, Pajevic PD, and Wu JY. PTH Signaling in Osteoprogenitors Is Essential for B-Lymphocyte Differentiation and Mobilization. J Bone Miner Res 2015; 30(12):2273-86.
6. Wu J, Purton LE, Rodda SJ, Chen M, Weinstein LS, McMahon AP, . . . Kronenberg HM. Osteoblastic regulation of B lymphopoiesis is mediated by Gsalpha-dependent signaling pathways. Proc Natl Acad Sci U S A 2008; 105(44):16976-81.
7. Schipani E, Kruse K, and Juppner H. A constitutively active mutant PTH-PTHrP receptor in Jansen-type metaphyseal chondrodysplasia. Science 1995; 268(5207):98-100.
8. Sinha P, Aarnisalo P, Chubb R, Poulton IJ, Guo J, Nachtrab G, . . . Wu JY. Loss of Gsalpha in the Postnatal Skeleton Leads to Low Bone Mass and a Blunted Response to Anabolic Parathyroid Hormone Therapy. J Biol Chem 2016; 291(4):1631-42.
9. Visnjic D, Kalajzic Z, Rowe DW, Katavic V, Lorenzo J, and Aguila HL. Hematopoiesis is severely altered in mice with an induced osteoblast deficiency. Blood 2004; 103(9):3258-64.
10. Rankin EB, Wu C, Khatri R, Wilson TL, Andersen R, Araldi E, . . . Giaccia AJ. The HIF signaling pathway in osteoblasts directly modulates erythropoiesis through the production of EPO. Cell 2012; 149(1):63-74.
11. Yu VW, Saez B, Cook C, Lotinun S, Pardo-Saganta A, Wang YH, . . . Scadden DT. Specific bone cells produce DLL4 to generate thymus-seeding progenitors from bone marrow. J Exp Med 2015; 212(5):759-74.
12. Fulzele K, Krause DS, Panaroni C, Saini V, Barry KJ, Liu X, . . . Divieti Pajevic P. Myelopoiesis is regulated by osteocytes through Gsalpha-dependent signaling. Blood 2013; 121(6):930-9.
13. Kobayashi T, Chung UI, Schipani E, Starbuck M, Karsenty G, Katagiri T, . . . Kronenberg HM. PTHrP and Indian hedgehog control differentiation of growth plate chondrocytes at multiple steps. Development 2002; 129(12):2977-86.
14. Rodda SJ and McMahon AP. Distinct roles for Hedgehog and canonical Wnt signaling in specification, differentiation and maintenance of osteoblast progenitors. Development 2006; 133(16):3231-44.
15. DeFalco J, Tomishima M, Liu H, Zhao C, Cai X, Marth JD, . . . Friedman JM. Virus-assisted mapping of neural inputs to a feeding center in the hypothalamus. Science 2001; 291(5513):2608-13.

16. Ding L, Saunders TL, Enikolopov G, and Morrison SJ. Endothelial and perivascular cells maintain haematopoietic stem cells. Nature 2012; 481(7382):457-62.
17. Pierini A, Nishikii H, Baker J, Kimura T, Kwon HS, Pan Y, . . . Negrin RS. Foxp3(+) regulatory T cells maintain the bone marrow microenvironment for B cell lymphopoiesis. Nat Commun 2017; 8:15068.
18. Kawamoto T. Use of a new adhesive film for the preparation of multi-purpose fresh-frozen sections from hard tissues, whole-animals, insects and plants. Arch Histol Cytol 2003; 66(2):123-43.
19. Kim JM, Rasmussen JP, and Rudensky AY. Regulatory T cells prevent catastrophic autoimmunity throughout the lifespan of mice. Nat Immunol 2007; 8(2):191-7.
20. Liu Y, Pop R, Sadegh C, Brugnara C, Haase VH, and Socolovsky M. Suppression of Fas-FasL coexpression by erythropoietin mediates erythroblast expansion during the erythropoietic stress response in vivo. Blood 2006; 108(1):123-33.
21. Socolovsky M, Nam H, Fleming MD, Haase VH, Brugnara C, and Lodish HF. Ineffective erythropoiesis in Stat5a(-/-)5b(-/-) mice due to decreased survival of early erythroblasts. Blood 2001; 98(12):3261-73.
22. Liu J, Zhang J, Ginzburg Y, Li H, Xue F, De Franceschi L, . . . An X. Quantitative analysis of murine terminal erythroid differentiation in vivo: novel method to study normal and disordered erythropoiesis. Blood 2013; 121(8):e43-9.
23. Acar M, Kocherlakota KS, Murphy MM, Peyer JG, Oguro H, Inra CN, . . . Morrison SJ. Deep imaging of bone marrow shows non-dividing stem cells are mainly perisinusoidal. Nature 2015; 526(7571):126-30.
24. Pietras EM, Reynaud D, Kang YA, Carlin D, Calero-Nieto FJ, Leavitt AD, . . . Passegue E. Functionally Distinct Subsets of Lineage-Biased Multipotent Progenitors Control Blood Production in Normal and Regenerative Conditions. Cell Stem Cell 2015; 17(1):35-46.
25. Yang L, Bryder D, Adolfsson J, Nygren J, Mansson R, Sigvardsson M, and Jacobsen SE. Identification of Lin(-)Sca1(+)kit(+)CD34(+)Flt3- short-term hematopoietic stem cells capable of rapidly reconstituting and rescuing myeloablated transplant recipients. Blood 2005; 105(7):2717-23.
26. Adolfsson J, Mansson R, Buza-Vidas N, Hultquist A, Liuba K, Jensen CT, . . . Jacobsen SE. Identification of Flt3+ lympho-myeloid stem cells lacking erythro-megakaryocytic potential a revised road map for adult blood lineage commitment. Cell 2005; 121(2):295-306.
27. Kondo M, Weissman IL, and Akashi K. Identification of clonogenic common lymphoid progenitors in mouse bone marrow. Cell 1997; 91(5):661-72.
28. Akashi K, Traver D, Miyamoto T, and Weissman IL. A clonogenic common myeloid progenitor that gives rise to all myeloid lineages. Nature 2000; 404(6774):193-7.
29. Pronk CJ, Rossi DJ, Mansson R, Attema JL, Norddahl GL, Chan CK, . . . Bryder D. Elucidation of the phenotypic, functional, and molecular topography of a myeloerythroid progenitor cell hierarchy. Cell Stem Cell 2007; 1(4):428-42.
30. Ding L and Morrison SJ. Haematopoietic stem cells and early lymphoid progenitors occupy distinct bone marrow niches. Nature 2013; 495(7440):231-5.

31. Greenbaum A, Hsu YM, Day RB, Schuettpelz LG, Christopher MJ, Borgerding JN, . . . Link DC. CXCL12 in early mesenchymal progenitors is required for haematopoietic stem-cell maintenance. Nature 2013; 495(7440):227-30.
32. Zhou BO, Yue R, Murphy MM, Peyer JG, and Morrison SJ. Leptin-receptor-expressing mesenchymal stromal cells represent the main source of bone formed by adult bone marrow. Cell Stem Cell 2014; 15(2):154-68.
33. Yang M, Arai A, Udagawa N, Hiraga T, Lijuan Z, Ito S, . . . Mizoguchi T. Osteogenic Factor Runx2 Marks a Subset of Leptin Receptor-Positive Cells that Sit Atop the Bone Marrow Stromal Cell Hierarchy. Sci Rep 2017; 7(1):4928.
34. Mizoguchi T, Pinho S, Ahmed J, Kunisaki Y, Hanoun M, Mendelson A, . . . Frenette PS. Osterix marks distinct waves of primitive and definitive stromal progenitors during bone marrow development. Dev Cell 2014; 29(3):340-9.
35. Inra CN, Zhou BO, Acar M, Murphy MM, Richardson J, Zhao Z, and Morrison SJ. A perisinusoidal niche for extramedullary haematopoiesis in the spleen. Nature 2015; 527(7579):466-71.
36. Liu Q, Li Z, Gao JL, Wan W, Ganesan S, McDermott DH, and Murphy PM. CXCR4 antagonist AMD3100 redistributes leukocytes from primary immune organs to secondary immune organs, lung, and blood in mice. Eur J Immunol 2015; 45(6):1855-67.
37. Stein JV and Nombela-Arrieta C. Chemokine control of lymphocyte trafficking: a general overview. Immunology 2005; 116(1):1-12.
38. Lo CG, Lu TT, and Cyster JG. Integrin-dependence of lymphocyte entry into the splenic white pulp. J Exp Med 2003; 197(3):353-61.
39. Mazo IB, Massberg S, and von Andrian UH. Hematopoietic stem and progenitor cell trafficking. Trends Immunol 2011; 32(10):493-503.
40. Sadahira Y, Yoshino T, and Monobe Y. Very late activation antigen 4-vascular cell adhesion molecule 1 interaction is involved in the formation of erythroblastic islands. J Exp Med 1995; 181(1):411-5.
41. Swami S, Johnson J, Bettinson LA, Kimura T, Zhu H, Albertelli MA, . . . Wu JY. Prevention of breast cancer skeletal metastases with parathyroid hormone. JCI Insight 2017; 2(17).
42. Fujii Y, Fujii K, Nakano K, and Tanaka Y. Crosslinking of CD44 on human osteoblastic cells upregulates ICAM-1 and VCAM-1. FEBS Lett 2003; 539(1-3):45-50.
43. Tanaka Y, Morimoto I, Nakano Y, Okada Y, Hirota S, Nomura S, . . . Eto S. Osteoblasts are regulated by the cellular adhesion through ICAM-1 and VCAM-1. J Bone Miner Res 1995; 10(10):1462-9.
44. Swarthout JT, D'Alonzo RC, Selvamurugan N, and Partridge NC. Parathyroid hormone-dependent signaling pathways regulating genes in bone cells. Gene 2002; 282(1-2):1-17.
45. Bellido T, Ali AA, Gubrij I, Plotkin LI, Fu Q, O'Brien CA, . . . Jilka RL. Chronic elevation of parathyroid hormone in mice reduces expression of sclerostin by osteocytes: a novel mechanism for hormonal control of osteoblastogenesis. Endocrinology 2005; 146(11):4577-83.
46. Keller H and Kneissel M. SOST is a target gene for PTH in bone. Bone 2005; 37(2):148-58.
47. Leupin O, Kramer I, Collette NM, Loots GG, Natt F, Kneissel M, and Keller H. Control of the SOST bone enhancer by PTH using MEF2 transcription factors. J Bone Miner Res 2007; 22(12):1957-67.

48. Wein MN, Spatz J, Nishimori S, Doench J, Root D, Babij P, . . . Kronenberg HM. HDAC5 controls MEF2C-driven sclerostin expression in osteocytes. J Bone Miner Res 2015; 30(3):400-11.
49. Lehrke M, Kahles F, Makowska A, Tilstam PV, Diebold S, Marx J, . . . Findeisen HM. PDE4 inhibition reduces neointima formation and inhibits VCAM-1 expression and histone methylation in an Epac-dependent manner. J Mol Cell Cardiol 2015; 81:23-33.
50. Ooi JY, Tuano NK, Rafehi H, Gao XM, Ziemann M, Du XJ, and El-Osta A. HDAC inhibition attenuates cardiac hypertrophy by acetylation and deacetylation of target genes. Epigenetics 2015; 10(5):418-30.
51. Malhotra S and Kincade PW. Canonical Wnt pathway signaling suppresses VCAM-1 expression by marrow stromal and hematopoietic cells. Exp Hematol 2009; 37(1):19-30.
52. Inoue K, Kobayashi M, Yano K, Miura M, Izumi A, Mataki C, . . . Minami T. Histone deacetylase inhibitor reduces monocyte adhesion to endothelium through the suppression of vascular cell adhesion molecule-1 expression. Arterioscler Thromb Vasc Biol 2006; 26(12):2652-9.
53. Lee CW, Lin CC, Luo SF, Lee HC, Lee IT, Aird WC, . . . Yang CM. Tumor necrosis factor-alpha enhances neutrophil adhesiveness: induction of vascular cell adhesion molecule-1 via activation of Akt and CaM kinase II and modifications of histone acetyltransferase and histone deacetylase 4 in human tracheal smooth muscle cells. Mol Pharmacol 2008; 73(5):1454-64.
54. Luo SF, Chang CC, Lee IT, Lee CW, Lin WN, Lin CC, and Yang CM. Activation of ROS/NF-kappaB and Ca2+/CaM kinase II are necessary for VCAM-1 induction in IL-1beta-treated human tracheal smooth muscle cells. Toxicol Appl Pharmacol 2009; 237(1):8-21.
55. Lin CC, Pan CS, Wang CY, Liu SW, Hsiao LD, and Yang CM. Tumor necrosis factor-alpha induces VCAM-1-mediated inflammation via c-Src-dependent transactivation of EGF receptors in human cardiac fibroblasts. J Biomed Sci 2015; 22:53.
56. Lamprou M, Kaspiris A, Panagiotopoulos E, Giannoudis PV, and Papadimitriou E. The role of pleiotrophin in bone repair. Injury 2014; 45(12):1816-23.
57. Liang T, Gao W, Zhu L, Ren J, Yao H, Wang K, and Shi D. TIMP-1 inhibits proliferation and osteogenic differentiation of hBMSCs through Wnt/beta-catenin signaling. Biosci Rep 2019; 39(1).
58. Gong W, Liu Y, Wu Z, Wang S, Qiu G, and Lin S. Meteorin-Like Shows Unique Expression Pattern in Bone and Its Overexpression Inhibits Osteoblast Differentiation. PLoS One 2016; 11(10):e0164446.
59. Yue R, Shen B, and Morrison SJ. Clec11a/osteolectin is an osteogenic growth factor that promotes the maintenance of the adult skeleton. Elife 2016; 5.
60. Martinez-Herrero S, Larrayoz IM, Ochoa-Callejero L, Fernandez LJ, Allueva A, Ochoa I, and Martinez A. Prevention of Bone Loss in a Model of Postmenopausal Osteoporosis through Adrenomedullin Inhibition. Front Physiol 2016; 7:280.
61. Kanai Y, Yasoda A, Mori KP, Watanabe-Takano H, Nagai-Okatani C, Yamashita Y, . . . Inagaki N. Circulating osteocrin stimulates bone growth by limiting C-type natriuretic peptide clearance. J Clin Invest 2017; 127(11):4136-4147.

62. Thomas G, Moffatt P, Salois P, Gaumond MH, Gingras R, Godin E, . . . Lanctot C. Osteocrin, a novel bone-specific secreted protein that modulates the osteoblast phenotype. J Biol Chem 2003; 278(50):50563-71.
63. Himburg HA, Termini CM, Schlussel L, Kan J, Li M, Zhao L, . . . Chute JP. Distinct Bone Marrow Sources of Pleiotrophin Control Hematopoietic Stem Cell Maintenance and Regeneration. Cell Stem Cell 2018; 23(3):370-381 e5.
64. Keller CC, Ouma C, Ouma Y, Awandare GA, Davenport GC, Were T, . . . Perkins DJ. Suppression of a novel hematopoietic mediator in children with severe malarial anemia. Infect Immun 2009; 77(9):3864-71.
65. Ouma C, Keller CC, Davenport GC, Were T, Konah S, Otieno MF, . . . Perkins DJ. A novel functional variant in the stem cell growth factor promoter protects against severe malarial anemia. Infect Immun 2010; 78(1):453-60.
66. Zhang J, Cohen A, Shen B, Du L, Tasdogan A, Zhao Z, . . . Morrison SJ. The effect of parathyroid hormone on osteogenesis is mediated partly by osteolectin. Proc Natl Acad Sci U S A 2021; 118(25).
67. Freedman MH and Saunders EF. Hematopoiesis in the human spleen. Am J Hematol 1981; 11(3):271-5.
68. Montague N and De La Ossa M. Massive splenomegaly and extramedullary hematopoiesis in chronic idiopathic myelofibrosis. Blood 2010; 116(14):2410.
69. Zewdu R, Risolino M, Barbulescu A, Ramalingam P, Butler JM, and Selleri L. Spleen hypoplasia leads to abnormal stress hematopoiesis in mice with loss of Pbx homeoproteins in splenic mesenchyme. J Anat 2016; 229(1):153-69.
70. Paulson RF, Shi L, and Wu DC. Stress erythropoiesis: new signals and new stress progenitor cells. Curr Opin Hematol 2011; 18(3):139-45.
71. Chen L, Wang J, Liu J, Wang H, Hillyer CD, Blanc L, . . . Mohandas N. Dynamic changes in murine erythropoiesis from birth to adulthood: implications for the study of murine models of anemia. Blood Adv 2021; 5(1):16-25.
72. Chen J, Shi Y, Regan J, Karuppaiah K, Ornitz DM, and Long F. Osx-Cre targets multiple cell types besides osteoblast lineage in postnatal mice. PLoS One 2014; 9(1):e85161.
73. Baccin C, Al-Sabah J, Velten L, Helbling PM, Grunschlager F, Hernandez-Malmierca P, . . . Haas S. Combined single-cell and spatial transcriptomics reveal the molecular, cellular and spatial bone marrow niche organization. Nat Cell Biol 2020; 22(1):38-48.
74. Tikhonova AN, Dolgalev I, Hu H, Sivaraj KK, Hoxha E, Cuesta-Dominguez A, . . . Aifantis I. The bone marrow microenvironment at single-cell resolution. Nature 2019; 569(7755):222-228.
75. Osunkwo I. An update on the recent literature on sickle cell bone disease. Curr Opin Endocrinol Diabetes Obes 2013; 20(6):539-46.
76. Vogiatzi MG, Macklin EA, Fung EB, Cheung AM, Vichinsky E, Olivieri N, . . . Thalassemia Clinical Research N. Bone disease in thalassemia: a frequent and still unresolved problem. J Bone Miner Res 2009; 24(3):543-57.
77. Valderrabano RJ, Lui LY, Lee J, Cummings SR, Orwoll ES, Hoffman AR, . . . Osteoporotic Fractures in Men Study Research G. Bone Density Loss Is Associated with Blood Cell Counts. J Bone Miner Res 2016.

78. Valderrabano RJ, Lee J, Lui LY, Hoffman AR, Cummings SR, Orwoll ES, . . . Osteoporotic Fractures in Men Study Research G. Older Men With Anemia Have Increased Fracture Risk Independent of Bone Mineral Density. J Clin Endocrinol Metab 2017; 102(7):2199-2206.

Figure Legends

Figure 1. Deletion of PTH1R in osteoprogenitors alters the distribution of mature hematopoietic lineages at 3 weeks of age. (A) Numbers of myeloid cells (B220-CD11b+CD3-Ter119-), T cells (B220-CD11b-CD3+Ter119-), B cells (B220+CD11b-CD3-Ter119-), and erythroid cells (B220-CD11b-CD3-Ter119+) in the bone marrow (left) and spleen (right) of PTH1R-OsxKO (KO, gray) and control (black) mice (n = 9 each). (B) Numbers of myeloid granulocyte subset (CD3-CD19-Ter119-CD11b+Ly6G+SiglecF-), monocyte/macrophage subset (CD3-CD19-Ter119-CD11b+Ly6G-SiglecF-), and eosinophil subset (CD3-CD19-Ter119-CD11b+SiglecF+) cells (n = 6 each). (C) Numbers of T cell CD4 (CD4+CD8-Foxp3-), CD8 (CD4-CD8+ Foxp3-), and regulatory T cell (Treg, CD4+Foxp3+) subsets (n = 4 each). (D) Numbers of erythroblast (EB) stages I through IV in bone marrow and spleen of PTH1R-OsxKO and control mice (n = 9 each). (E) Circulating white blood cells, but not red blood cells or platelets, are decreased in the peripheral blood of PTH1R-OsxKO mice. Red blood cell (RBC), hemoglobin (Hb), mean corpuscular volume (MCV), (F) white blood cell (WBC), lymphocyte (lymph), monocyte (mono), neutrophil (neu), (G) platelet (PLT) (n = 11 each).

Figure 2. Deletion of PTH1R in osteoprogenitors has no effect on hematopoietic stem and progenitor cells in the bone marrow. (A) Numbers of long-term HSCs (LT-HSC, CD150+CD48-Lin-c-kit+Sca-1+), short-term HSCs (ST-HSC, CD34+Flt3-Lin-c-kit+Sca-1+), lymphoid-primed MPPs (LMPP, CD34+Flt3+Lin-c-kit+Sca-1+), common lymphoid progenitors (CLP, CD127+Lin-c-kit+Sca-1+), common myeloid progenitors (CMP, CD34+CD16/32-Lin-c-kit+Sca-1-), megakaryocyte-erythrocyte progenitors (MEP, CD34-CD16/32-Lin-c-kit+Sca-1-), or granulocyte-monocyte progenitors (GMP, CD34+CD16/32+Lin-c-kit+Sca-1-) in the bone marrow (left) and spleen (right) of KO (gray) and control (black) mice at 3 weeks of age (n = 10 each). (B) Numbers of pre-GM (CD41-CD16/32-CD150-CD105-), GMP (CD41-/CD150-/CD16/32+), pre-MegE (CD41-CD16/32-CD150+CD105-), pre-CFU-E (CD41-CD16/32-CD150+CD105+), CFU-E (CD41-CD16/32-CD150-CD105+Ter119-), pro-Ery (CD41-CD16/32-CD150-CD105+Ter119+) and MkP (CD41+ CD150+) (n = 4 each). (C) Numbers of CFU-E and BFU-E in bone marrow and spleen (n = 3 each). (D) Thymus

weight (mg), thymus weight (mg) per gram body weight (g), thymus cellularity, and thymus cellularity per gram body weight in KO and control mice at 3 weeks of age (n = 4 each). (E) Numbers of T cell precursors double negative (DN, Lin-CD4-CD8-), DN1 (Lin-CD4-CD8-CD25-CD44+), DN2 (Lin-CD4-CD8-CD25+CD44+), DN3 (Lin-CD4-CD8-CD25+CD44-), DN4 (Lin-CD4-CD8-CD25-CD44-), double positive (DP, Lin-CD4+CD8+), CD4 single positive (SP, Lin-CD4+CD8-) and CD8 SP (Lin-CD4-CD8+) in the thymus of KO and control mice (n = 4 each).

Figure 3. Proliferation is decreased in multiple hematopoietic lineages in PTH1R-OsxKO mice. (A) Distribution of myeloid (My), T cell (T), B cell (B), and erythroid (Er) populations among cell cycle stages G0, G1, and G2/M/S in bone marrow and spleen of control (black) and KO (gray) mice at 3 weeks of age (n = 3 each). (B) Distribution of erythroblast (EB) stage I through IV cells among cell cycle stages G0, G1, and G2/M/S in bone marrow and spleen of control and KO mice (n = 4 each). (C) Immunostaining for Ter119 (green) and Ki-67 (white) in the bone marrow of KO and control mice at 3 weeks. Scale bar = 500 μm (upper panels) and 50 μm (lower panels). (D) Immunostaining for Ter119, B220 (red), and Ki-67 in the spleen of KO and control mice at 3 weeks. Scale bar = 1 mm.

Figure 4. Osteoprogenitors expressing osterix are present in bone, while descendants of osterix-expressing osteoprogenitors are present in bone and bone marrow. (A) Immunostaining of GFP+ osterix-expressing osteoprogenitors and Tomato+ descendants in femur of Osx-Cre::GFP/+; PTH1R(+/+); Ai14/+ (PTH1R-OsxWT) control and Cre::GFP/+; PTH1R(fl/fl); Ai14/+ (PTH1R-OsxKO) mice at 3 weeks of age. Scale bar = 500 μm (left panels) and 100 μm (right panels). (B) Representative flow cytometry detection of GFP+ and GFP-Tomato+ cells in bone and bone marrow of PTH1R-OsxWT and PTH1R-OsxKO mice. (C) Frequencies and numbers of GFP+ and GFP-Tomato+ cells in bone marrow and bone of PTH1R-OsxWT (n = 11) and PTH1R-OsxKO (n = 9) mice.

Figure 5. Osx-expressing osteoprogenitors give rise to distinct populations in bone and bone marrow. (A) PCA plot of PTH1R-OsxWT (WT) and PTH1R-OsxKO (KO) BM-historic (BM-H), bone-current (bone-C), and bone-historic (bone-H) populations using the rlog-transformed values of RNA-seq data. Each color represents a sample type. Each sample has three replicates. (B) Heatmap of relative log transformed values of total genes across samples. Each row represents a gene. Each column represents a cell type. (C) Relative expression levels of *Pth1r*, *Vcam1*, and *Cxcl12* in bone marrow-historic, bone-current, and bone-historic populations. Adjusted *p* values for *Pth1r*: 4.87E-08 (BM-H), 7.96E-04 (bone-C), 9.20E-05 (bone-H); for *Vcam1*: 5.66E-19 (BM-H), 4.98E-27 (bone-C), 2.83E-68 (bone-H); for *Cxcl12*: 1.63E-04 (BM-H), 1.09E-33 (bone-C), 3.09E-36 (bone-H). (D) Percent of myeloid (My), T, B, and erythroid (Er) cells expressing VCAM-1 and VLA-4 in bone marrow of PTH1R-OsxKO (KO, gray) and control (black) mice (n = 5 each).

Figure 6. Differentially expressed niche factors. (A) Top 20 niche factor transcripts that are significantly upregulated in PTH1R-OsxWT BM-historic (BM-H), bone-current (bone-C), and bone-historic (bone-H) populations. –log10 (p value) of gene-enriched terms are shown. (B) Top 20 niche factor transcripts that are significantly upregulated in PTH1R-OsxKO BM-H, bone-C, bone-H populations.

Supplementary Figure Legends

Supplementary Figure 1. The Osx-Cre::GFP transgene is not expressed in the spleen at 3 weeks. (A) Immunostaining for Osx-GFP (green) and CD31 (red) in bone of Osx-Cre::GFP/+ mice at 3 weeks. Scale bar = 500 μm. (B) Immunostaining for Osx-GFP (green), CD45 (red), and CD31 (cyan) in the spleen of Osx-Cre::GFP/+ mice at 3 weeks. Scale bar = 1 mm.

Supplementary Figure 2. Erythroblast stage IV and erythrocyte stages V and VI are increased in the bone marrow of PTH1R-OsxKO mice. (A) Flow cytometry phenotyping protocol for erythroblast stages I-IV) [20, 21]. (B) Flow cytometry phenotyping protocol for erythroblast stages I and IV and erythrocyte stages V and VI [22]. (C) Numbers of erythroblast (EB) stages I through IV and erythrocyte stages V and VI in bone marrow and spleen of PTH1R-OsxKO and control mice (n = 9 each).

Supplementary Figure 3. Deletion of PTH1R in LepR-Cre-expressing mesenchymal progenitors does not affect hematopoiesis. (A) Body weight, bone marrow cellularity, spleen weight, and spleen cellularity in PTH1R-LepRKO (gray) and control (black) mice at 3 months (n = 3-4 each). (B) Numbers of myeloid (My), T, B, erythroid (Er) and erythroblast (EB) stage I to IV populations in bone marrow and spleen of PTH1R-LepRKO and control mice at 3 months (n = 3-4 each). (C) Body weight, bone marrow cellularity, spleen weight, and spleen cellularity in PTH1R-LepRKO and control mice at 12 months (n = 7 each). (D) Numbers of myeloid (My), T, B, erythroid (Er) and erythroblast (EB) stage I to IV populations in bone marrow and spleen of PTH1R-LepRKO and control at 12 months (n = 7 each).

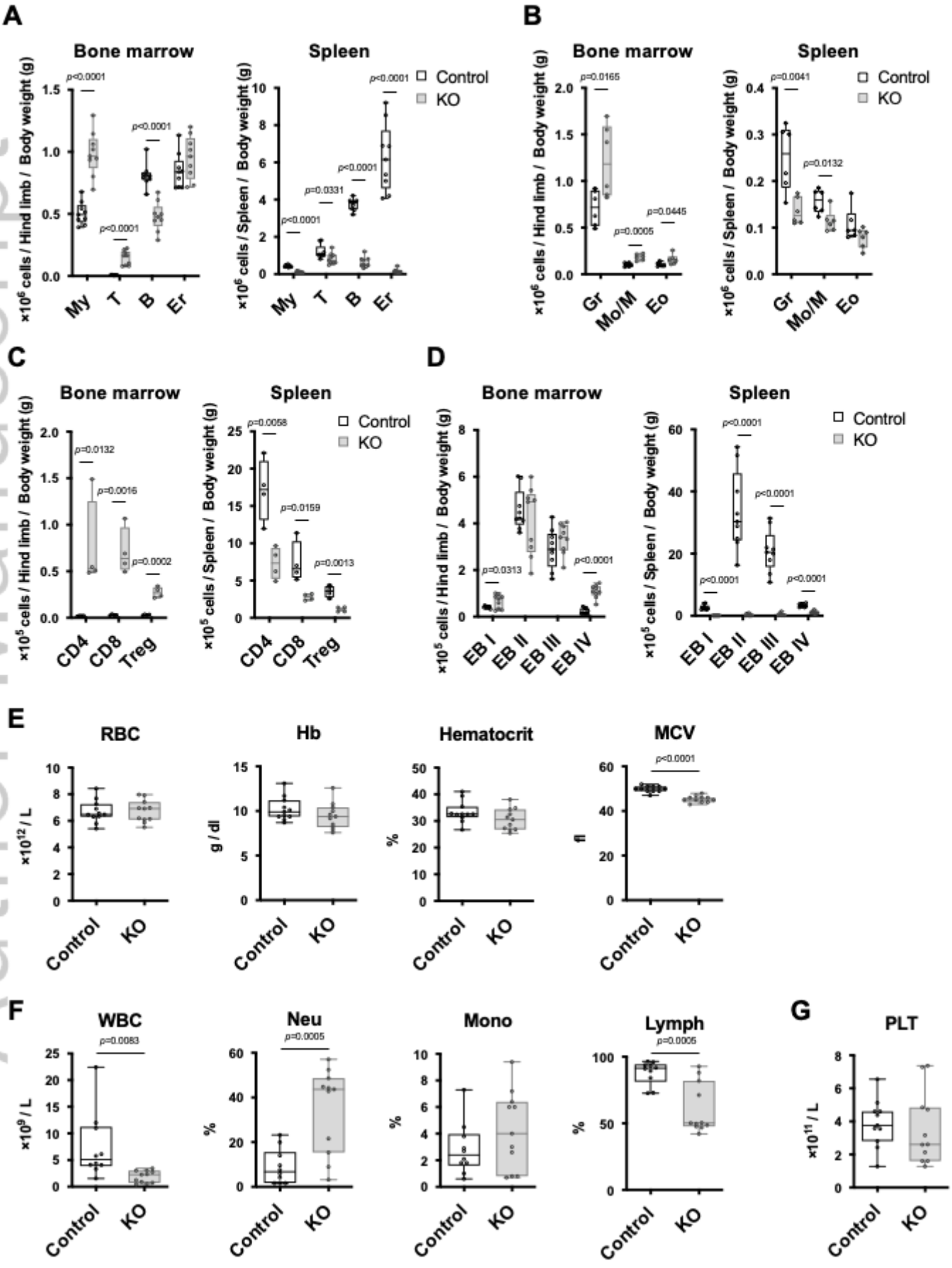

JBMR_4568_Figure 1.tiff

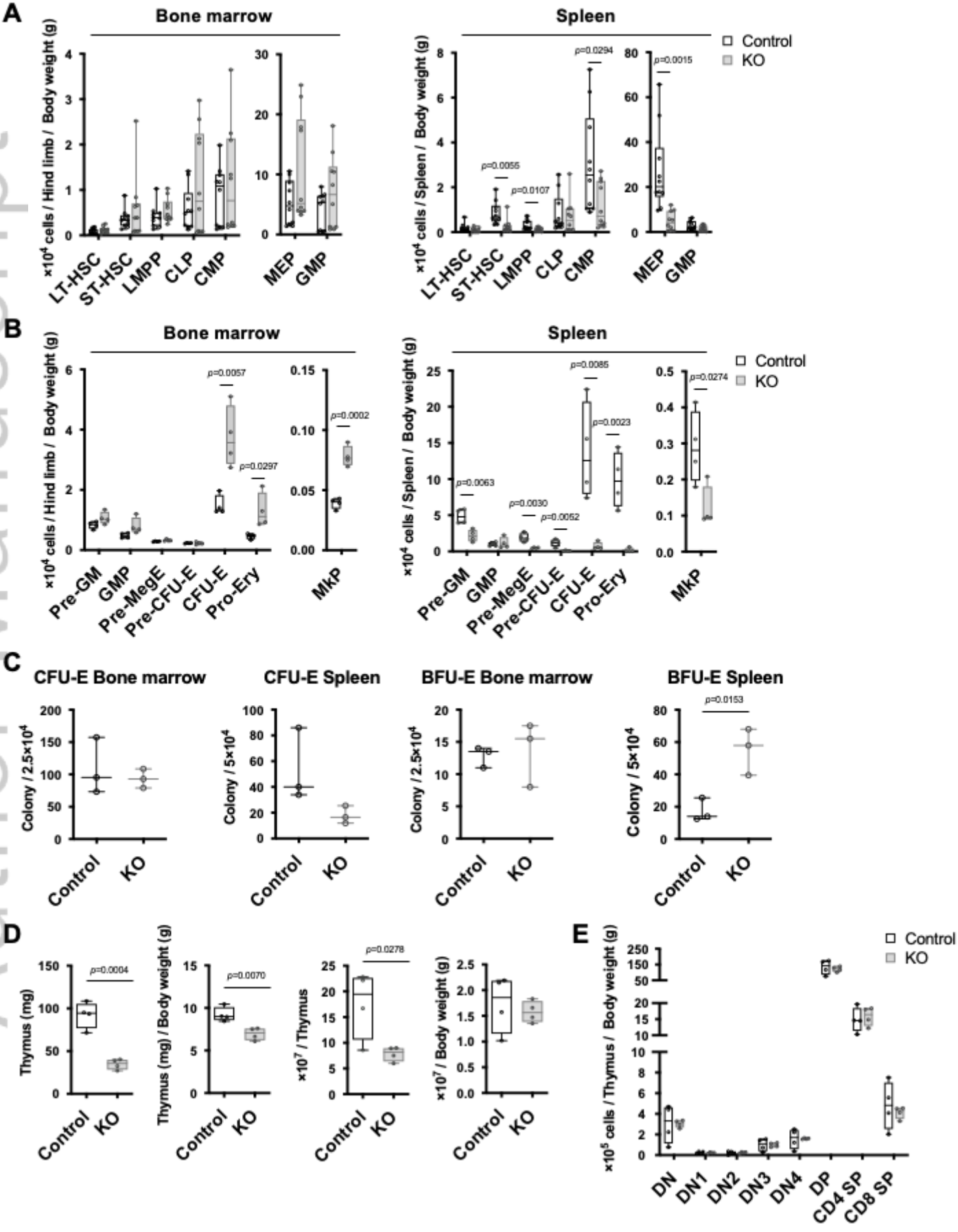

JBMR_4568_Figure 2.tiff

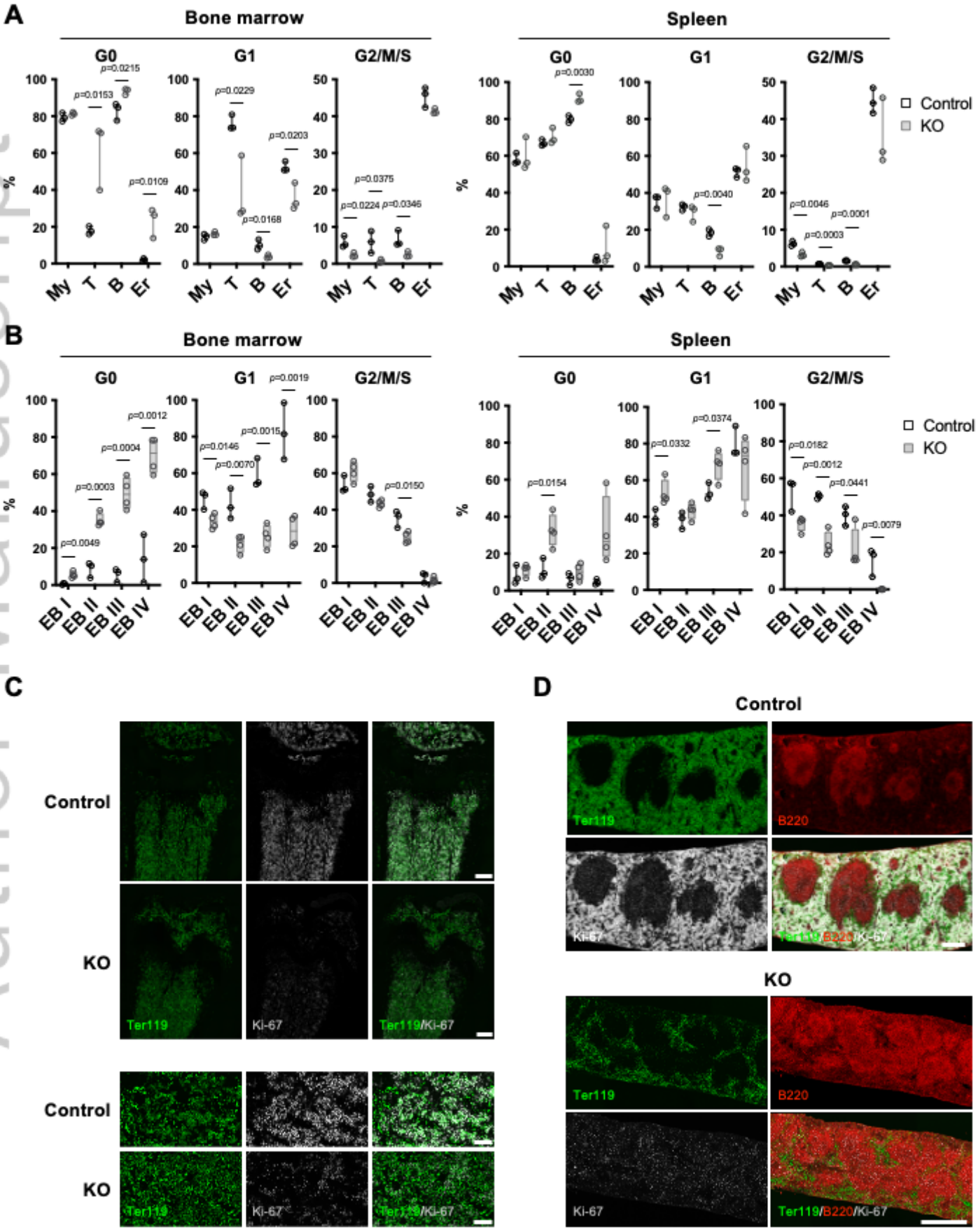

JBMR_4568_Figure 3.tiff

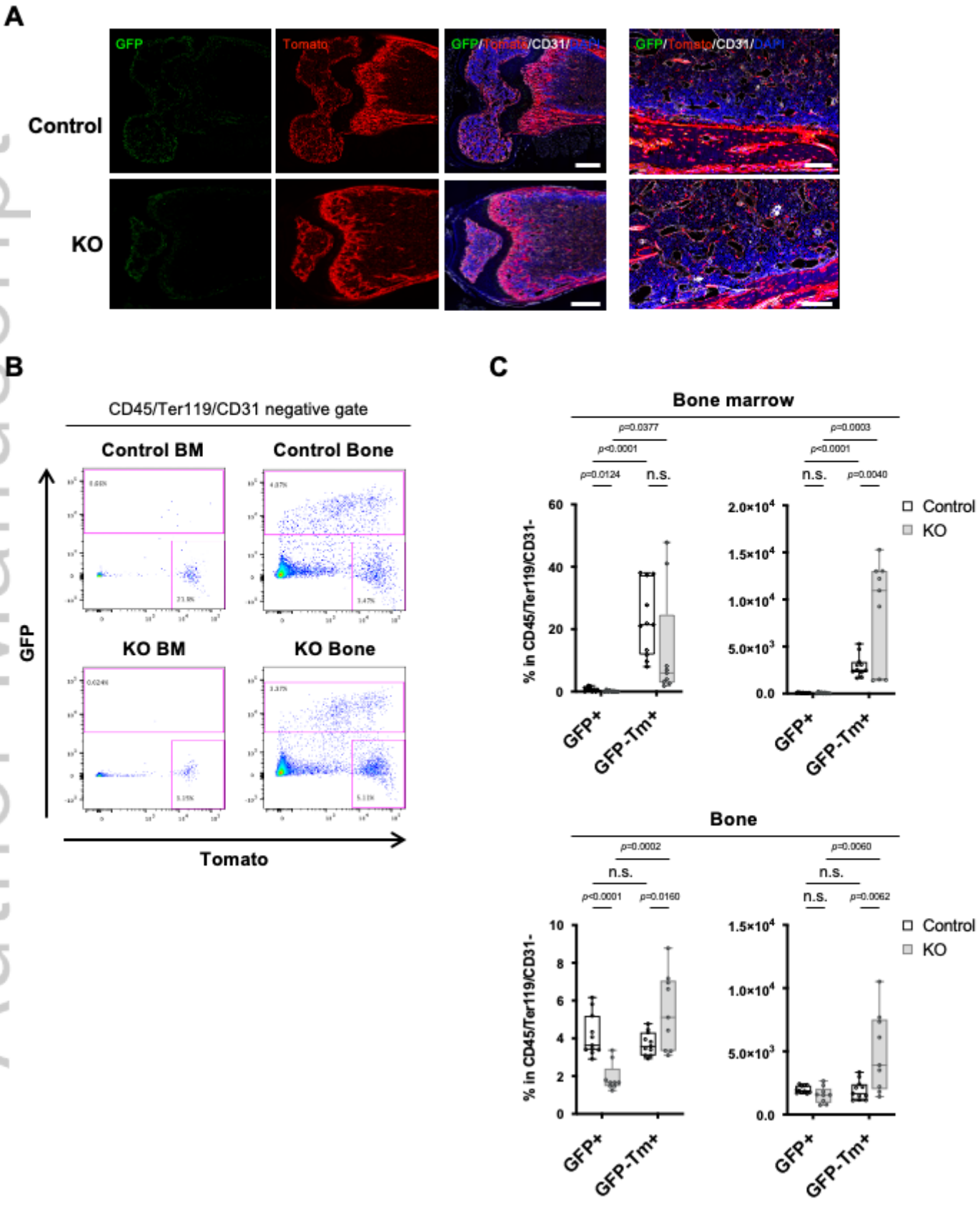

JBMR_4568_Figure 4.tiff

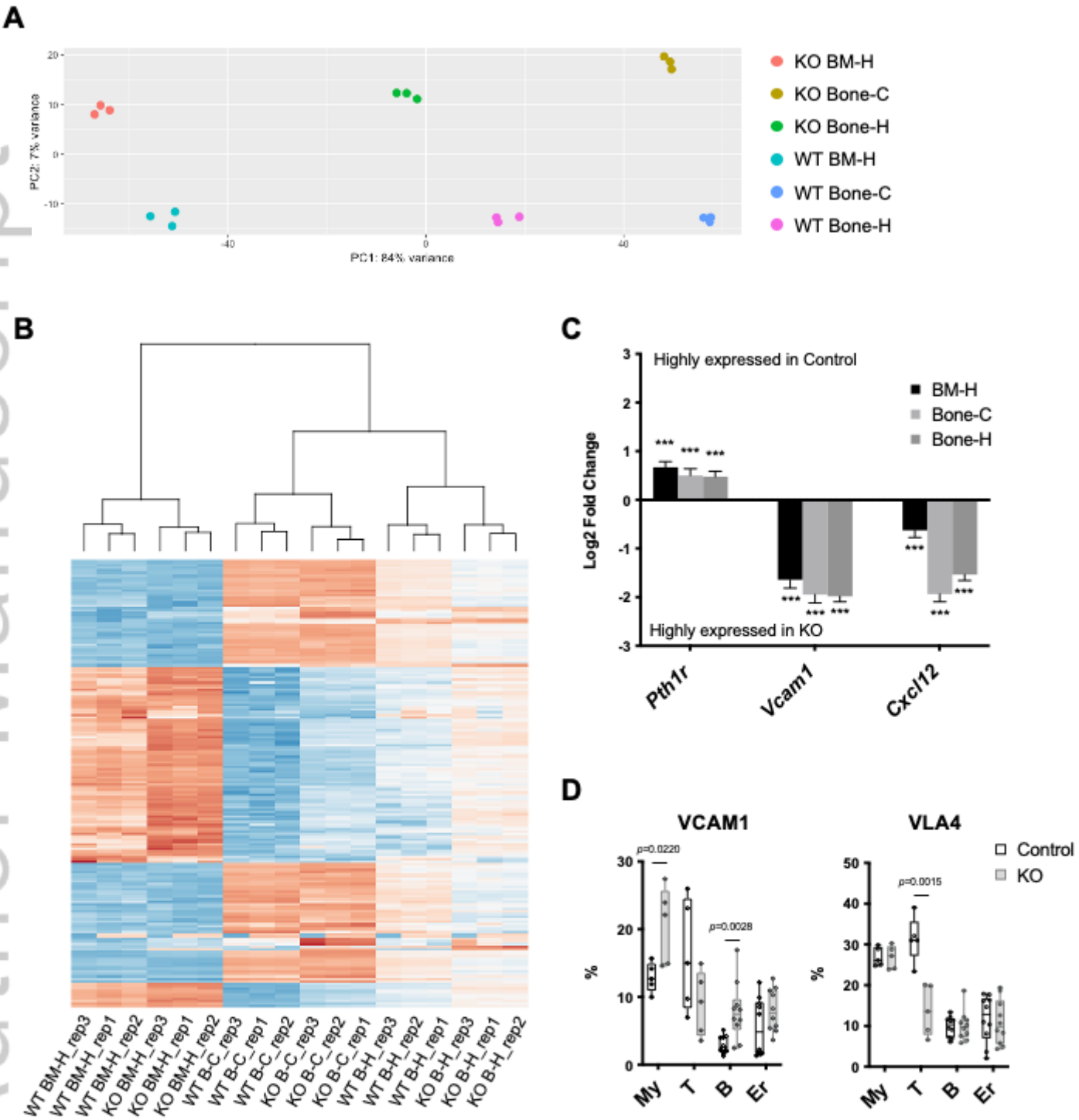

JBMR_4568_Figure 5.tiff

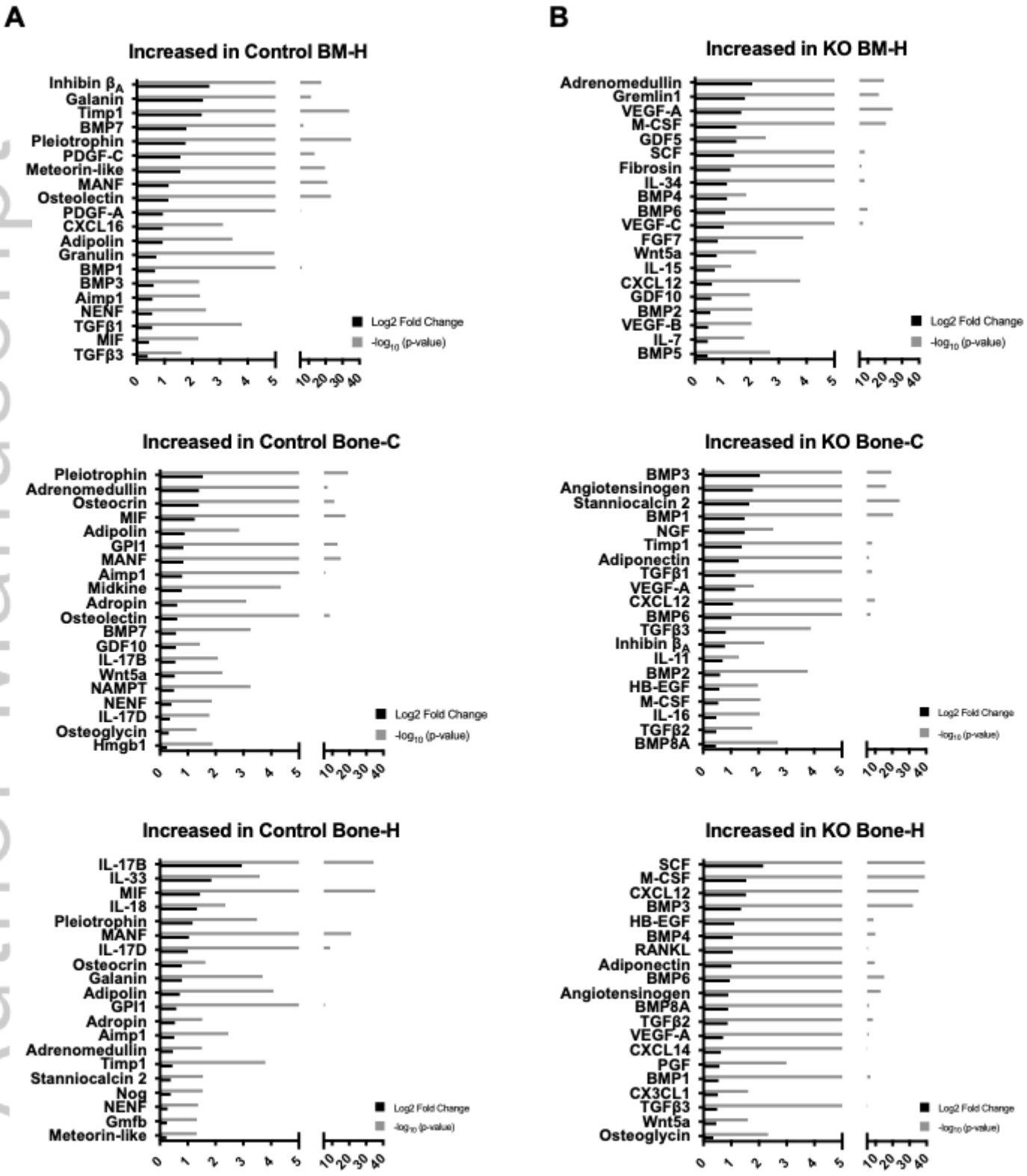

JBMR_4568_Figure 6.tiff